AIAA 2003–4095

Comparison of Three Geometric Representations of Airfoils for Aerodynamic Optimization

Hsiao-Yuan Wu, Shuchi Yang, and Feng Liu
Department of Mechanical and Aerospace Engineering
University of California, Irvine, CA 92697-3975

Her-Mann Tsai
Temasek Laboratories
National University of Singapore
Kent Ridge Crescent, Singapore 119260

16th AIAA Computational Fluid Dynamics Conference
June 23–26, 2003/Orlando, FL

Comparison of Three Geometric Representations of Airfoils for Aerodynamic Optimization

Hsiao-Yuan Wu,* Shuchi Yang,† and Feng Liu‡
Department of Mechanical and Aerospace Engineering
University of California, Irvine, CA 92697-3975

Her-Mann Tsai§
Temasek Laboratories
National University of Singapore
Kent Ridge Crescent, Singapore 119260

Three geometric representation methods for airfoils are compared for the design and optimization of turbomachinery cascades by an adjoint equation method. They are the PARSEC method, the Hicks-Henne shape function method, and the mesh-point method. Two-dimensional, transonic, and inviscid inverse design problems are studied. Comparisons are made for three different configurations including the NACA0015 airfoil, the 10th standard configuration compressor blade, and the VKI turbine nozzle blade. Gradient information for optimization is obtained by using a continuous adjoint equation method based on the Euler equations. Conjugate gradient method is adopted as the optimization scheme. The results suggest that the PARSEC method is not suitable for representing cascade blade shapes, the Hicks-Henne shape function method converges to the optimum faster than the mesh-point method does, but the mesh-point method can reach higher accuracy.

I Introduction

Several geometric representation methods have been used to describe the shapes of airfoils, such as the Joukowski transformation, polynomial representations, B-spline curves, and etc. Discrete points are used to describe airfoil shapes in CFD applications. Given an arbitrary airfoil shape, how well a method can approach the shape depends on the completeness of the set of all the shapes the method can describe. In an aerodynamic optimization problem the optimum design is an unknown shape, and the performance of the optimization process depends on how well the geometry representation method can approach the optimum shape. Intuitively, a method with more design parameters should have a more complete set of shapes, and therefore can approach the design target better.

During the optimization process, gradient of the cost function is needed for each design cycle in order to improve the design. With a finite-difference method, the computational cost for obtaining gradient information is proportional to the number of design parameters. Therefore, one has to be limited to the use of a small number of design parameters. However, if an adjoint equation method is applied, the computational cost for obtaining the gradient information is essentially independent of the number of design parameters. Therefore, one can ignore the concern about the computational cost for the gradient when choosing the geometric representation method for optimization and design.

Many works have been done on aerodynamic optimization and design using a few different geometric representation methods. However, these works have different design objectives, flow and geometric configurations, , optimization schemes, and etc. Their performances cannot be compared directly to show which geometric representation method is better.

In this study, three geometric representation methods for 2-D airfoils are compared under the same conditions, so that the influences of the representation methods can be discussed. They are the PARSEC[1] method, the Hicks-Henne shape function method,[2,3] and the mesh-point method.[4] The comparisons are made for three transonic inverse design cases. Emphasis is focused on turbomachinery blade design. Known

*Graduate Researcher, AIAA Student Member.

†Post-doctoral Researcher.

‡Associate Professor, AIAA Member.

§Principal Research Scientist, AIAA Member.

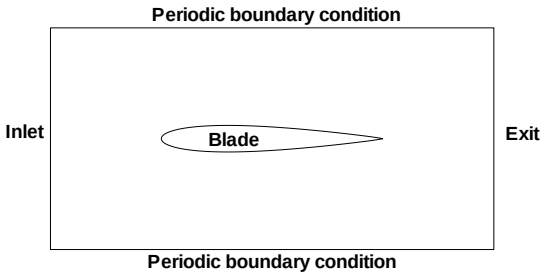

Fig. 1 Domain of a cascade blade passage

airfoil shapes including the NACA0015 airfoil, the 10th standard configuration compressor blade,[5,6] and the VKI turbine nozzle blade[7,8] are used as the design targets, and therefore the accuracies of design can be measured by comparing the results with the known targets.

The authors developed an optimization code[9] based on the adjoint equation method for the Euler equations. A conjugate gradient method[10] is used as the optimization scheme in this paper. Since the computational cost for the flow evaluation and gradient calculation is almost the same for all three geometric representation methods, the number of design cycles needed to reach the optimum point is used as a measure of the speed of a method. Although each method behaves differently in different test cases, the relative performances of the three methods are quite consistent for all three cases.

II Inverse Design as an Optimization Problem.

Inverse design problems of two-dimensional turbomachinery cascades are studied based on the Euler equations. Figure 1 is a sketch of the domain. Periodic boundary conditions are applied on the upper boundary and the lower boundary. At the inlet, the stagnation pressure, the stagnation density, and the angle of the flow are specified. At the exit, the static pressure is specified. A target pressure distribution p_d is given on the blade. The design purpose is to modify the initial blade shape to obtain the target pressure distribution. The cost function is defined as:

$$I = \frac{1}{2}\int_{B_W}(p - p_d)^2 dB_W \qquad (1)$$

in which B_W is the blade surface, p is the actual pressure. A smaller value of the cost function means the design is closer to the target design.

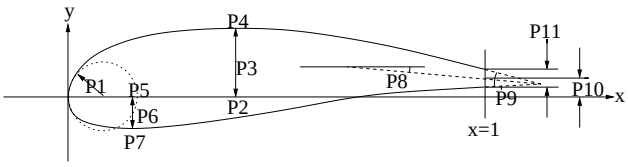

Fig. 2 The PARSEC representation method

III Description of the Three Geometric Representation Methods.

Three geometric representation methods for two-dimensional airfoil shapes are studied. They are the PARSEC method, the Hicks-Henne shape function method, and the mesh-point method. The details for these methods are described below.

A The PARSEC method.

This method uses 11 parameters to represent an airfoil.[1] They are the leading edge radius (P_1), upper crest position (P_2, P_3), upper crest curvature (P_4), lower crest position (P_5, P_6), lower crest curvature (P_7), trailing edge direction (P_8), trailing edge wedge angle (P_9), trailing edge offset (P_{10}), and trailing edge thickness (P_{11}). They are shown in Figure 2. The mathematical formulation for the PARSEC is:

$$y_u = \sum_{n=1}^{6} a_n x^{n-\frac{1}{2}} \quad ,$$

$$y_l = \sum_{n=1}^{6} b_n x^{n-\frac{1}{2}} \quad , \qquad (2)$$

where y_u is the coordinate of the upper surface and y_l is that of the lower surface, x is the chordwise location. The chord length is assumed to be 1, and a_n and b_n are coefficients to be solved by using the 11 given parameters.

B The Hicks-Henne Shape Function Method.[2,3]

The shape functions are defined as

$$b_i(x) = sin^4(\pi x^{m_i}) \quad , \qquad m_i = ln(0.5)/ln(x_{Mi})$$

$$i = 1, 2, ..., 32,$$

where x is the chordwise coordinate and $0 \le x \le 1$, x_{Mi} are pre-selected values corresponding to the locations of the maxima b_i. In this specific case, there are 16 Hicks-Henne shape functions for the upper surface and 16 for the lower surface, respectively. For the first two test cases, the locations of x_{Mi} for $i = 1, 2, ..., 16$ are chosen to be $0.5 \times [1 - cos(\theta_i)]$, where $\theta_i = \pi \times i/17$. For $i = 17, 18, ..., 32$, x_{Mi}=x_{Mj}, and $j = i - 16$. The distribution is denser near the leading edge and the trailing edge. For the VKI turbine nozzle case, x is the normalized arc length from the leading edge, and

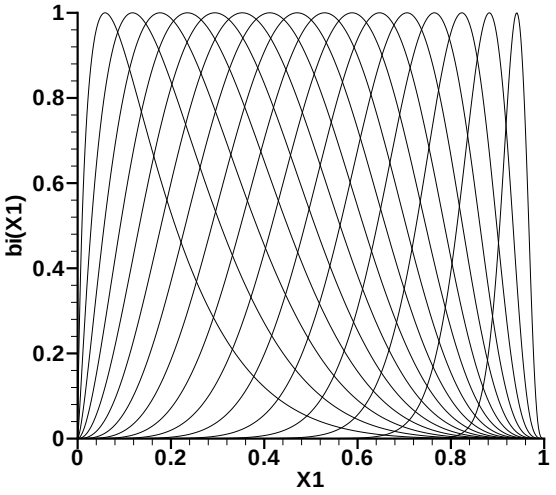

Fig. 3 The Hicks-Henne shape functions

the locations of x_{Mi} are uniformly distributed. Figure 3 shows the shape of these functions. They are added to an initial airfoil shape to form a new shape. The weight of these shape functions are then the design parameters.

C The Mesh Point Method.

For a numerical computation, mesh points are used to represent the airfoil surface. The mesh-point method uses the coordinates of these points directly as the design parameters. In this paper, there are 160 vertex points on the surface for the first two test cases and 192 vertex points for the last test case. For the first two cases, the x_1 coordinates of all surface points are fixed, and only the x_2 coordinates can be modified according to the gradient information. For the last test case, both x_1 and x_2 coordinates can be modified during the design process.

IV Gradient Information for Optimization

A continuous adjoint equation method based on the Euler equations developed by the authors in Ref. 10 is applied to obtain the gradient information for the optimization design. For all three methods, the adjoint equations and the corresponding boundary conditions are the same. The computational time needed for the solution of the adjoint equations is independent of the number of design parameters. After the adjoint equations are solved, however, different procedures are applied to calculate the gradient. The computational time for this part is negligible compared to the flow and adjoint equation evaluations. Therefore the overall computational time for obtaining the gradient information is essentially independent of the number of design parameters.

For the PARSEC method, the 11 variables are perturbed one at a time. For each perturbation δP_k, a new set of coefficients a_n and b_n are obtained by solving a linear system based on the known PARSEC variables, and then the shape is calculated according to Equation (2). Each time the blade shape is perturbed, the mesh needs to be adjusted once. The new mesh is obtained by linear interpolation.[11] After the new shape and mesh are obtained, the variation of the cost function δI is calculated by using the adjoint variables and geometric variations. Then the gradient for this specific PARSEC variable is obtained as $\delta I_k/\delta P_k$, no summation convention on k is applied.

For the Hicks-Henne shape function method, the gradient information is obtained as the following. Small bump functions are added to an initial airfoil shape one at a time. The bump functions are

$$\delta y_\beta(x) = (\delta c_\beta) \cdot b_\beta(x),$$

(no summation convention on β is applied.)

in which $\beta = 1, 2, ..., 32$, δc_β is the size of perturbation, $b_\beta(x)$ is the β-th Hicks-Henne shape function. For each perturbation, the variation of the cost function is calculated by using the geometry variations and the adjoint variables and then the gradient is obtained.

For the mesh-point method, with the linear interpolation method for mesh adjustment, an analytical form of gradient for each mesh point can be derived. No perturbation of the shape is needed. During the design process, the locations of mesh points are modified according to the gradients. However, the gradient distribution on the blade surface is usually less smooth than the original blade shape. In order to maintain the smoothness of the shape, the gradient distribution needs to be smoothed before it is used to modify the shape. In this study, the Sobolev implicit smoothing scheme is applied.[12] For the VKI turbine nozzle case, mesh points are allowed to move in both the x_1 and x_2 directions. Two components of gradients are calculated for each mesh point, and the smoothing procedure is applied on the two components separately.

After the gradient information is obtained, conjugate gradients are calculated.[10] Along the conjugate gradient direction, a one-dimensional search method is applied to find an approximate minimum point. For the first of every 10 design cycles, the search direction is reset to the gradient direction in order to avoid error accumulation.

V Results and Discussions

Comparisons of the three geometric representation methods are made for three transonic inverse design cases. They are the NACA0015 cascade, the 10th

standard configuration compressor blade, and the VKI turbine nozzle blade. Two major factors are investigated: the speed of convergence to the optimum and the accuracy measured by the minimum achievable cost function values. During the design process, given the search direction and an estimated step size (the step size of the previous design cycle), if the program cannot find a better design, it halves the step size and evaluates the new design till a better design is obtained. In this study, if the step size is halved for more than 12 times in one design cycle, it is considered that the method has reached its limit and the program is stopped. The final value of the cost function is used as a measure of the accuracy of the method. The number of design cycles needed to reach the limit is used as a measure of the speed of convergence.

The flow solver and the adjoint solver are modified from Flo52x. A three-level multi-grid method and residual smoothing scheme are used to accelerate the computation. An implicit smoothing scheme is applied on the adjoint boundary condition to avoid discontinuities caused by shock waves.[4] The definition of the cost function is therefore modified, but when the new cost function is decreased to zero, the original cost function will also be zero. For computation inside the program, the modified cost function is used, but the original cost function as defined in Equation (1) is used for the output values.

A Comparisons for the NACA0015 Cascade Case

The first case is a cascade consisting of a series of the NACA0015 airfoils. It has a zero stagger angle and a unit space to chord ratio. Air enters the inlet with a zero degree angle of attack. A back pressure corresponding to an isentropic Mach number of 0.7 is specified. The mesh for this case is a 160×32 O-mesh and it is shown in Figure 4. The initial shape for the Hicks-Henne shape function method and the mesh-point method is the NACA0012 airfoil, while the initial shape for the PARSEC method is an approximation to the NACA0012 using PARSEC variables. For all three methods, the target pressure is the pressure distribution of the NACA0015 airfoil.

Figure 5 shows the history of the cost function for the three methods. The values are normalized by the cost function value of the initial NACA0012. The computations reach their minimum cost function values after 149 design cycles for the PARSEC method, 44 design cycles for the Hicks-Henne shape function method, and 197 design cycles for the mesh-point method. For transonic design cases, strong nonlinear flow behavior can possibly cause complicated structures of the cost function distribution in the design space. Since the mesh-point method has more free parameters, the structure of the cost function distribution is probably more complicated. Therefore the path leading to the optimum point is not as straight forward as that of the Hicks-Henne shape function method, and it may take more design cycles to reach the optimum point. For the PARSEC method, other than the nonlinear flow behavior, there are strong nonlinear factors of the geometric variations as well, and that may cause additional complication for the structure of the cost function distribution, and therefore slow down the speed of convergence. Moreover, the strong nonlinear behavior of geometric variations also mean that the perturbation sizes may significantly affect the accuracy of the gradient calculation. Figure 6 shows the relation between the magnitude of a gradient component and the perturbation size for calculating this component. For the Hicks-Henne shape function method, the component for the 8th shape function on the lower surface is examined, and the gradient component is hardly affected by the perturbation size. For the PARSEC method, the component for the lower crest location is examined, and the influence of perturbation size is obvious. This also means the perturbation sizes for the PARSEC method need to be carefully examined for each design parameter and they may need to be adjusted for different geometric configurations, which is not practical. In this case, the PARSEC method is slower than the Hicks-Henne shape function method even though it has fewer design parameters.

On the other hand, the mesh-point method can reach the highest accuracy (lowest cost function value) among the three methods. The Hicks-Henne shape function method is the second best. This is consistent with our expectation: the accuracy is proportional to the number of design parameters. More design parameters usually mean a more complete design space and hence a better capability of approaching the design target.

Figure 7 shows the comparison of blade shapes and Figure 8 shows the corresponding pressure distributions. Here the C_p is defined as $(p - p_b)/(p_0 - p_b)$, where p_b is the back pressure at the exit and p_0 is the total pressure at the inlet. Results of all three methods match the design target very well. There is hardly any visible deviations.

B Comparisons for the 10th Standard Configuration Compressor Blade

The second case is the 10th standard configuration.[5,6] It has a stagger angle of 45 degrees and a unit space to chord ratio. The inflow angle is 58 degrees (13 degrees with respect to the chord line). The design inlet Mach number is 0.8. The mesh for computation is shown in Figure 9. It is still a 160×32 O-mesh. For convenience, the chord line is aligned

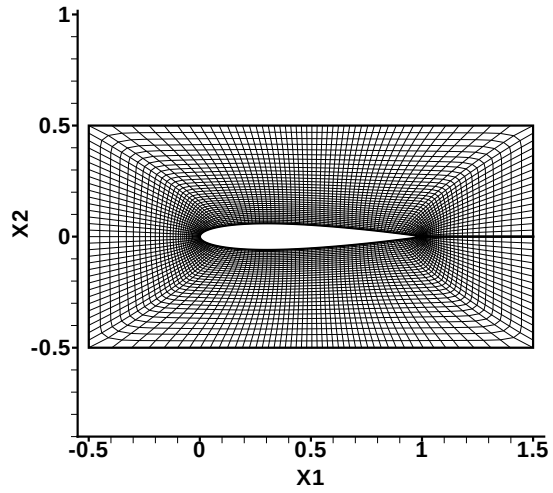

Fig. 4 Mesh for the NACA0015 cascade case.

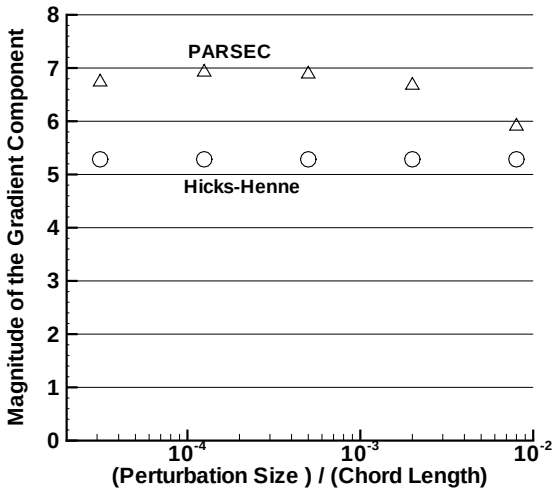

Fig. 6 Influences of the perturbation sizes on the gradient calculation.

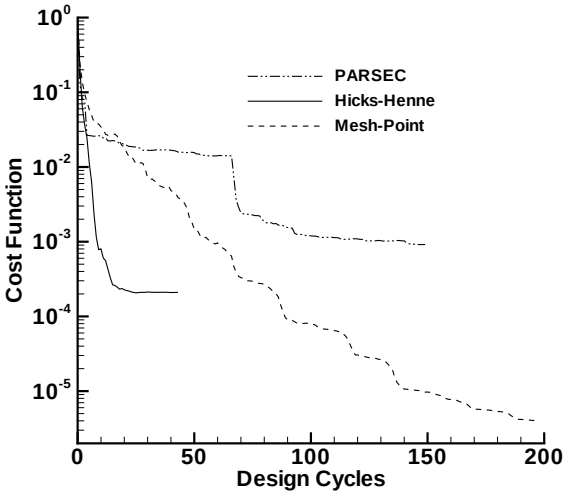

Fig. 5 History of the cost function for the NACA0015 cascade case.

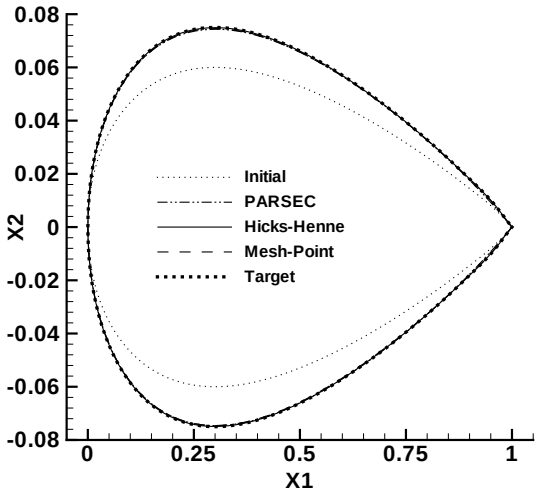

Fig. 7 Comparison of the blade shapes for the NACA0015 cascade case.

to the x_1 axis. The initial shape for the Hicks-Henne shape function method and the mesh-point method is a deformed 10th standard configuration shown in Figure 14. Sine waves with amplitudes of 1% chord length are superposed on the upper and lower surfaces of the target shape, respectively. However, when the same numerical method as the previous case is used to solve for the PARSEC representation for the initial shape, an extremely large deviation appears for the lower surface as shown in Figure 10. The reason is that when the PARSEC variables are converted to the a_n and b_n's in Equation (2), a linear system needs to be solved. The system includes coefficients like $x_c^{5.5}$ and $x_c^{-1.5}$, where x_c is the chordwise location of the crest (P_2 or P_5 in Figure 2). If $x_c << 1$, the above terms differ by orders of magnitude, resulting in an ill-conditioned linear system. The values of the PARSEC variables are obtained by curve fitting to the known vertex coordinates of the initial shape and there are numerical errors in this process. For the lower surface the crest is very close to the leading edge ($x_c << 1$), and therefore even small numerical errors can cause a large deviation of the shape. This means that the PARSEC method is not suitable for cascade blades because most of cascade blades have their crest locations very close to the leading edges. Under this condition, perturbing the PARSEC variables can cause a extremely large shape change, and accurate gradient information is difficult

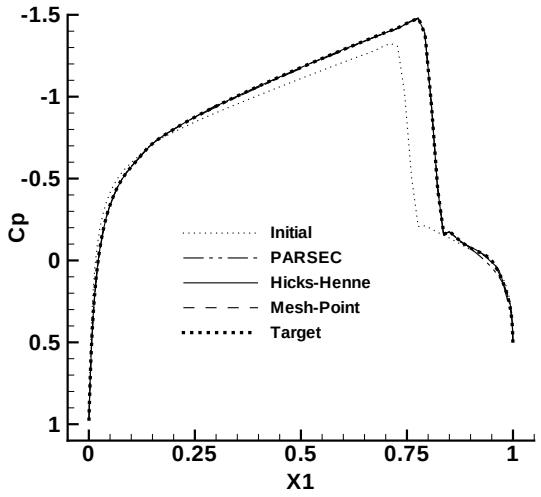

Fig. 8 Comparison of the C_p distributions for the NACA0015 cascade case.

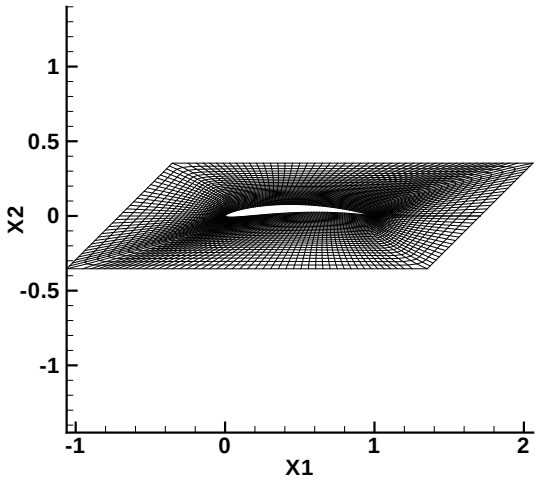

Fig. 9 Mesh for the 10th standard configuration case.

to obtain.

A PARSEC approximation of NACA0012 is used as the initial shape for the PARSEC method. The same set of perturbation sizes as the previous test case is used. At the 20th design cycle the program reaches its limit, but the cost function goes down for about only one order. The perturbation sizes suitable for the NACA0015 airfoil may not be suitable for this compressor blade. Comparisons of shapes and pressure distributions are shown in Figures 11 and 12, respectively. An unphysical shape is produced by this method and it is still far from the target shape. The pressure distribution is also very different from the target pressure distribution. Based on the results and discussions above, this method is considered not suitable for compressor blade design.

Figure 13 shows the history of the cost function for the Hicks-Henne shape function method and the mesh-point method. The Hicks-Henne shape function method reaches its limit at the 73rd design cycle. As in the previous test case, it has a higher speed of convergence than the mesh-point method. Compared to the NACA0015 cascade case, the cost function values decrease slower for both methods. However, the effect is more serious for the mesh-point method, and its cost function value hardly goes down for the last half of the design process. A major difference between this case and the previous case is that the expansion pressure gradient near the leading edge is stronger in this case, The mesh-point method may have problems to deal with strong pressure suction close to the leading edge. Fine tuning the smoothing procedure may be able to improve its performance. The mesh-point method is expected to reach a higher accuracy than that of the shape function method. However, in this case it falls behind the Hicks-Henne method for any practical purpose.

The best design of the Hicks-Henne shape function method (the result of the 73rd design cycle) is used as an initial condition for the mesh-point method to see if better design can be obtained. The result is also shown in Figure 13, the dashed curve continuing the solid curve of the Hicks-Henne method. While the shape function method has reached its minimum, the mesh-point method can further reduce the cost function value, although the speed is very slow. This is consistent with our expectation for the accuracy. It also suggests that a proper combination of the two method may have better performance than each method alone.

Figure 14 shows the shape of the best design of the Hicks-Henne method and that of 100 design cycles of the mesh-point method. The result of the combined Hicks-Henne and mesh-point method is not shown in the figure. It is closer to the target shape than the shape of the Hicks-Henne mehtod and the deviation from the target shape can hardly be seen. Figure 15 shows the C_p distributions corresponding to the shapes shown in Figure 14. The shape and pressure distribution of the Hicks-Henne shape function method is very close to the design target. The shape of the mesh-point method has not become close to the target shape after 100 design cycles. However, the deviation of the pressure distribution is much smaller than that of the shape. At the suction side the designed pressure distribution matches the target pressure distribution very well.

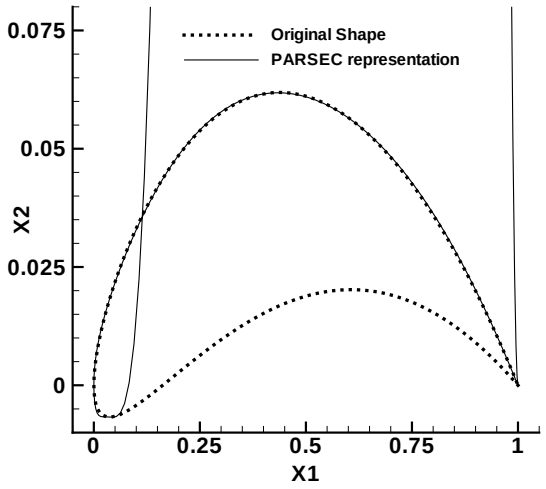

Fig. 10 Representing a compressor blade shape using the PARSEC method.

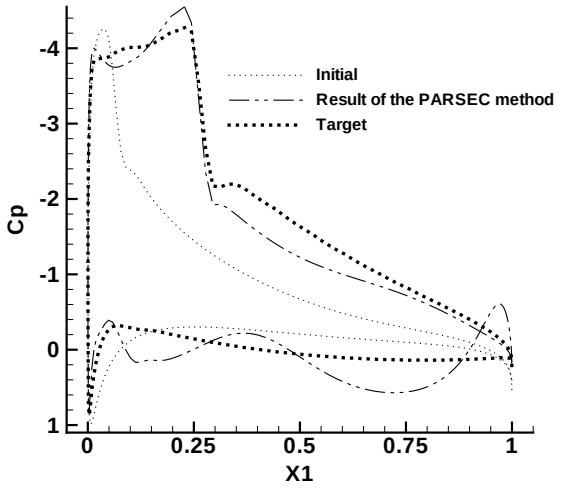

Fig. 12 C_p distributions of the PARSEC method for the 10th standard configuration case.

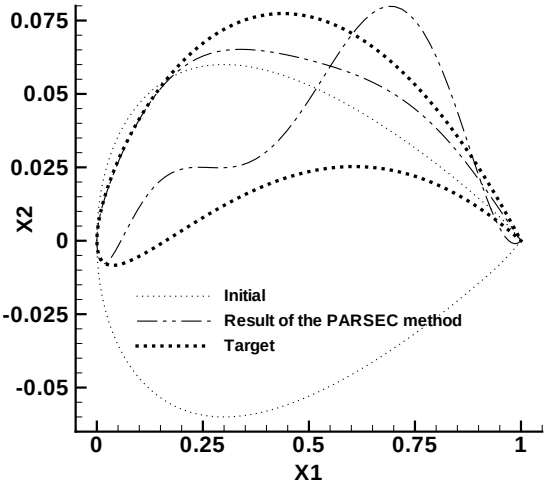

Fig. 11 Blade shapes of the PARSEC method for the 10th standard configuration case.

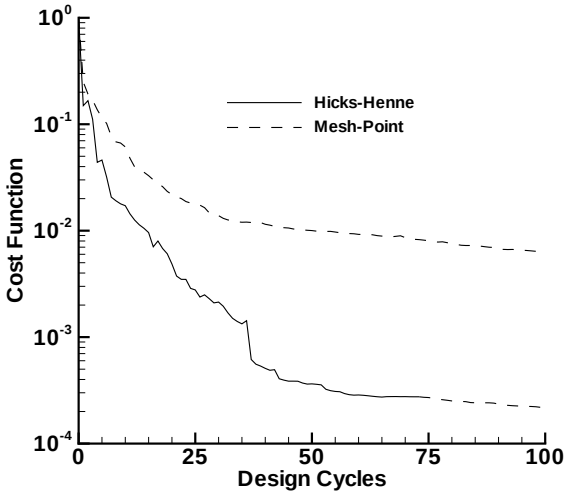

Fig. 13 History of the cost function for the 10th standard configuration case.

C Comparison for the VKI Turbine Nozzle Blade

The third case is the VKI turbine nozzle blade.[7,8] The inflow angle is 0 degree. The isentropic exit Mach number is 1.45. The mesh for the computation is shown in Figure 16. It is a 192×20 O-mesh. The chord line is defined to be a line tilted by 75 degrees with respect to the x_1 axis, and the leading edge is obtained accordingly.

Like other turbine blades, the VKI blade has a blunt trailing edge, and it causes problems for the Euler solver and the adjoint solver. Adding a sharp trailing edge can help the solvers' convergence, but the shape of the sharp trailing edge may significantly affect the flow field. Arbitrarily assigning a trailing edge shape may result in a blade which behaves quite differently from the original VKI blade. Therefore, a "soft cusp" is added to the trailing edge as shown in Figure 17. A soft cusp is equivalent to a large cell. Residuals are calculated and the flow variables inside the cusp are updated by a time marching method. Its boundary AC satisfies the solid wall boundary condition. It helps the solvers to converge and the flow field hardly depends on its shape. During the design process, the shape of the soft cusp is kept unchanged. The smoothing procedure for the boundary conditions of the adjoint

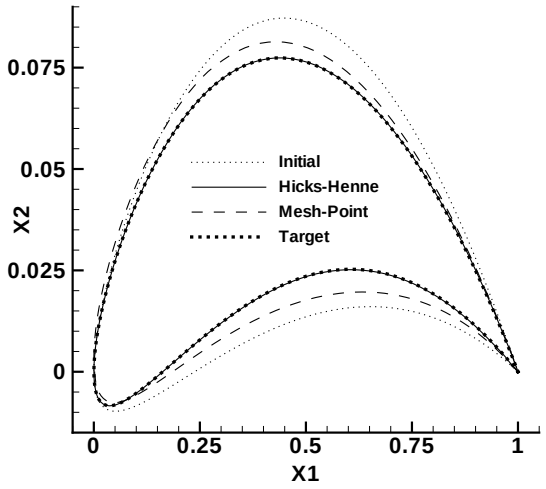

Fig. 14 Comparison of the blade shapes for the 10th standard configuration case.

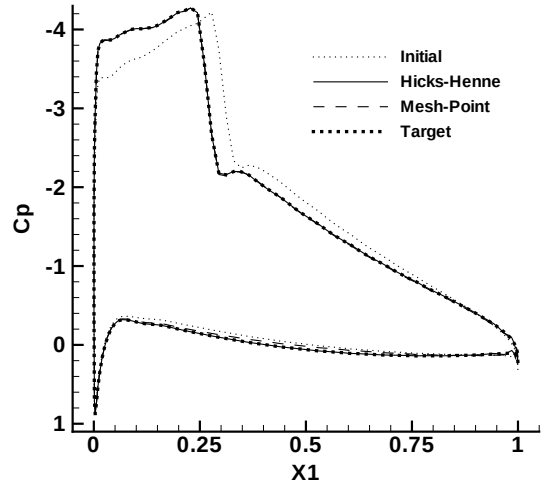

Fig. 15 Comparison of the C_p distributions for the 10th standard configuration case.

equations is deactivated due to this soft cusp. From Figure 17 and Figure 19 it can be seen that there is an unphysical suction peak at point A. To avoid the problems the suction peak may cause, a small section AD of the blade surface is kept unchanged for the initial shape, the target shape, and during the design process.

The initial shape for the Hicks-Henne shape function method and the mesh-point method is a deformed VKI blade: bump functions with the form of $sin^2(\pi s)$ are superposed to the upper and lower surfaces, where s is the normalized arc length from the leading edge. The displacements of the surface vertices are all along the normal directions of the target shape. For the Hicks-Henne shape function method, surface vertices are only allowed to move along the normal directions during the design process, while for the mesh-point method the vertices can move on both x_1 and x_2 directions. Similar to the previous case, there is a problem to represent the lower surface by using the PARSEC variables, so the lower crest location is moved to a location farther away from the leading edge to avoid the singularity. The initial shape for the PARSEC method is shown in Figure 18. The same perturbation sizes for gradient calculation as the previous two cases are used. The PARSEC method can at most decrease the cost function value for less than one order. The designed shape and the target shape are shown in Figure 18. The shape is not changed by much and only at the rear part of the pressure side has visible difference from the initial shape. This is different from the previous case. The initial shape has a lower crest location closer (15% chord length) to the leading edge than the previous case does (30% chord length), the shape may be much more sensitive to the perturbations, and thus the accuracy of the gradient is degraded. Therefore the improvement of the shape is quite limited. The corresponding pressure distributions are shown in Figure 19. The designed pressure distribution is still very different from the target pressure distribution. The PARSEC method is not suitable for this turbine blade configuration.

Figure 20 shows the history of the cost function for the Hicks-Henne shape function method and the mesh-point method. At the 162nd design cycle, the Hicks-Henne shape function method reaches its limit. It converges to its optimum faster than the mesh-point method does. For the last half of the design process, the mesh-point method becomes even slower in this case. In order to find out possible reasons that cause slow convergence speed, the x_2 components of the gradient for all mesh points are plotted with respect to their x_1 locations as shown in Figure 21. The magnitudes are normalized. At the first design cycle, the gradient is smooth. After 100 design cycles, the gradient has some fluctuation near the trailing edge on the suction side, and the fluctuation becomes more obvious at the 200th design cycle. The blade shape at the same location also becomes uneven. Even with the implicit smoothing scheme applied on the gradient, there is some mechanism that can amplify the fluctuation at the location as the number of design cycle increases. These fluctuations may cause the reduction of the step size of optimization and therefore slow down the convergence.

Again, the best design of the Hicks-Henne shape function method (the result of the 162nd design cycle) is used as an initial condition for the mesh-point method to see if better results can be obtained. The

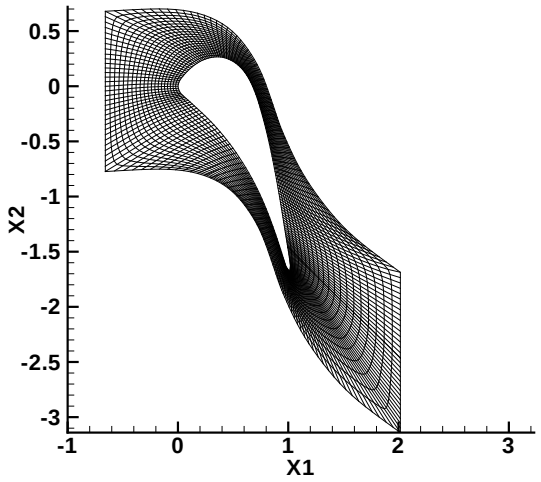

Fig. 16 Mesh for the VKI turbine nozzle case.

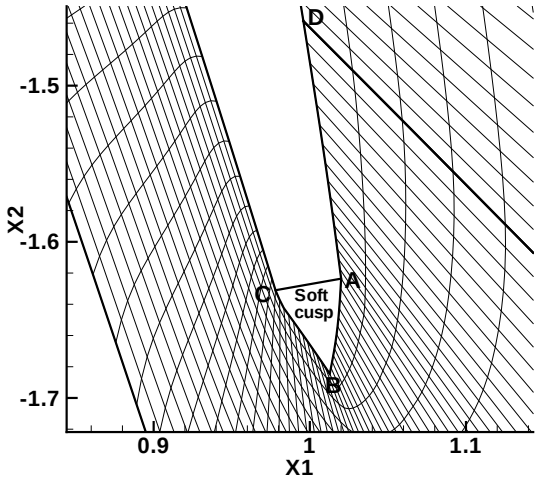

Fig. 17 The soft cusp.

result is also shown in Figure 20. The improvement is significant within the 38 additional design cycles. The cost function goes down for more than half an order. It shows the ability of the mesh-point method to reach higher accuracy than that of the shape function method. The relative performances between these two methods are consistent with the two previous test cases. Consider the history of the cost function after 162 design cycles in Figure 20. The additional computations with the mesh-point method on top of the converged solution by the Hicks-Henne method have a smooth starting shape and gradient, and the cost function goes down fast. Fine tuning the smoothing parameters to eliminate the fluctuations may be able to improve the performance of the mesh-point method.

Figure 22 shows the shape of the best design of the Hicks-Henne method and that of 200 design cycles of the mesh-point method. Again, the result of the combined Hicks-Henne and mesh-point method is not shown in the figure. It is closer to the target than the result of the Hicks-Henne method. Figure 23 shows the corresponding pressure distributions. The results of the shape function method match the design target very well. The deviations of the mesh-point method are slightly more obvious.

VI Conclusions

Three geometric representation methods are compared for aerodynamic design of cascade blades. They are the PARSEC method, the Hicks-Henne shape function method, and the mesh-point method. Their speeds of convergence to the optimum point and the accuracies are discussed. Three transonic inverse design problems including the NACA0015 cascade, the 10th standard configuration compressor blade, and the

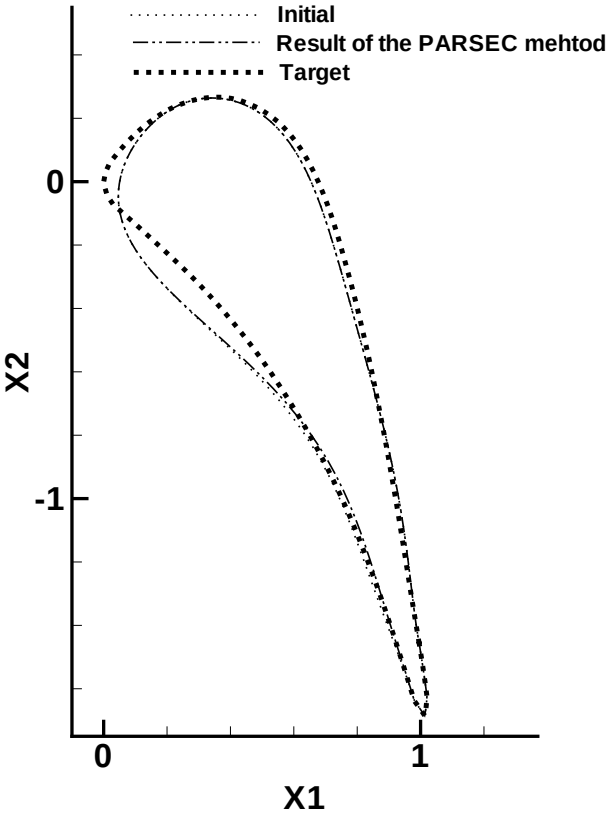

Fig. 18 Blade shapes of the PARSEC method for the VKI turbine nozzle case.

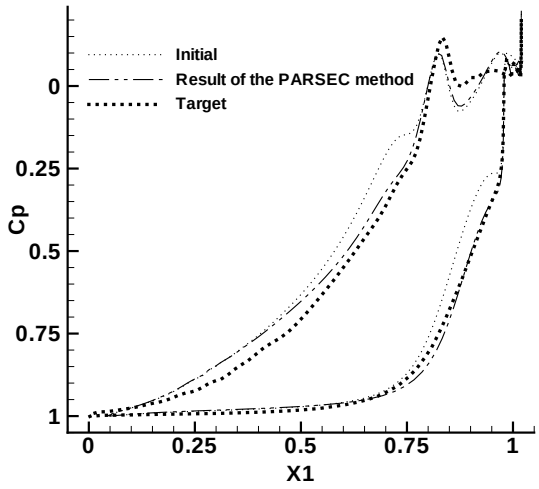

Fig. 19 C_p **distributions of the PARSEC method for the VKI turbine nozzle case.**

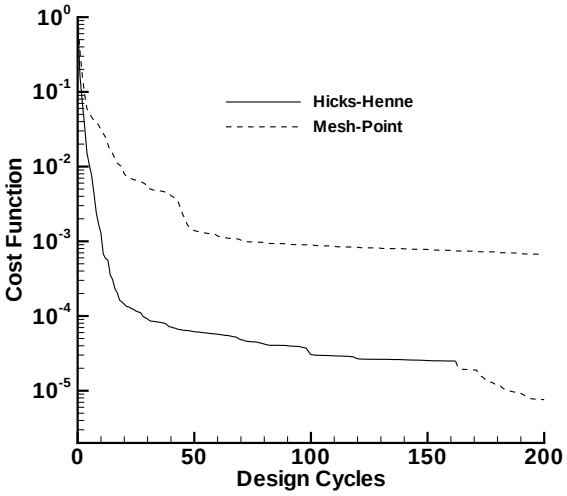

Fig. 20 History of the cost function for the VKI turbine nozzle case.

VKI turbine nozzle blade are studied. A continuous adjoint equation method based on the Euler equations is adopted to obtain the gradient for optimization.

The PARSEC method works reasonably well for the NACA0015 cascade case, but it is not suitable for compressor or turbine blade design. For all three test cases, the Hicks-Henne shape function method reaches its optimum faster than the mesh-point method does. For the NACA0015 case, the mesh-point method can reach a higher accuracy than that of the shape function method within a reasonable number of design cycles. This is consistent with our expectation that a method with more design parameters should be able to reach a higher accuracy. On the other hand, for the com-

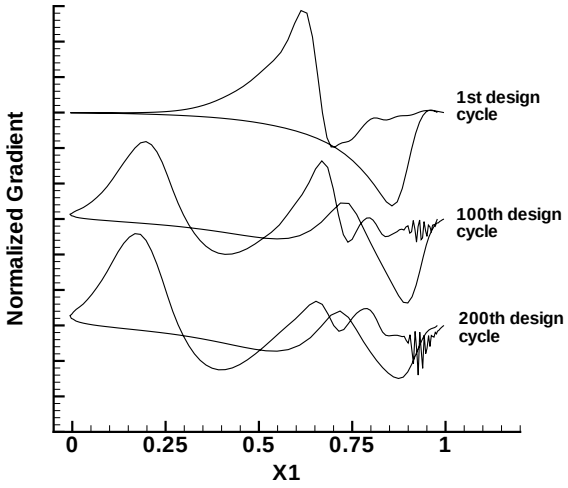

Fig. 21 Gradient of the mesh-point method for the VKI turbine nozzle case.

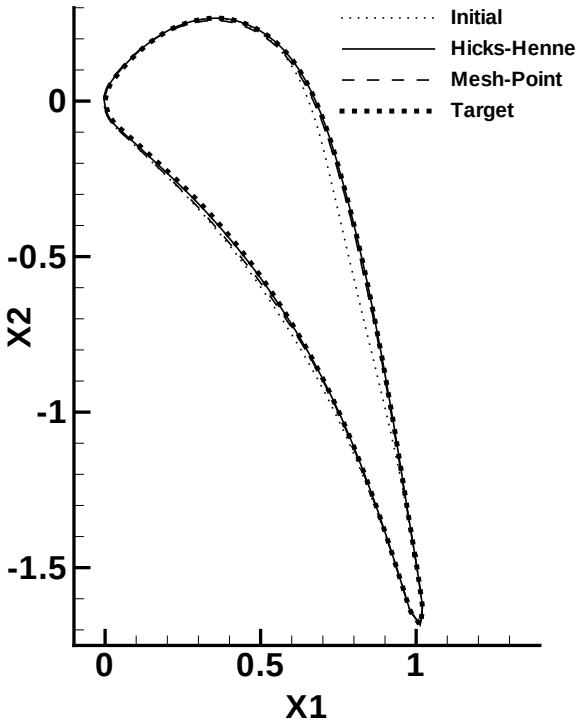

Fig. 22 Comparison of the blade shapes for the VKI turbine nozzle case.

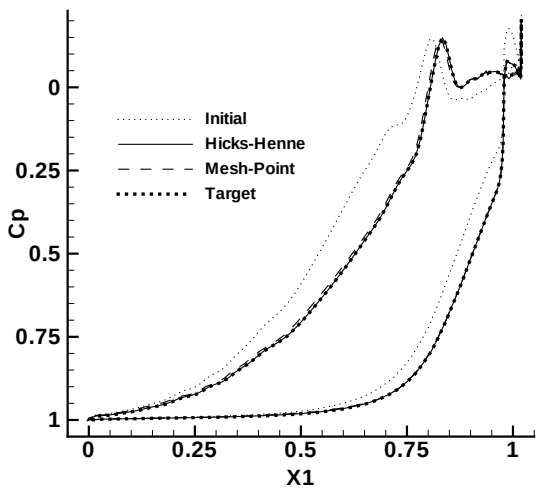

Fig. 23 Comparison of the C_p distributions for the VKI turbine nozzle case.

pressor and VKI blade cases, the mesh-point method becomes much slower, and it needs much more design cycles than the shape function method does to reach the optimum point. However, it is shown that the mesh-point method can further improve the best design of the Hicks-Henne shape function method to reach higher accuracies. The smoothing procedure of the gradient may affect the performance of the mesh-point method.

References

[1]Sobieczky, H., "Parametric Airfoils and Wings," *Notes on Numerical Fluid Mechanics*, 1998, pp. 71–88.

[2]Hicks, R. and Henne, P., "Wing Design by Numerical Optimization," *Journal of Aircraft*, Vol. 15, No. 7, 1978, pp. 407–413.

[3]Reuther, J., "Aerodynamic Shape Optimization Using Control Theory," NASA Technical Report NASA-CR-201064, 1996.

[4]Jameson, A., "Optimum Aerodynamic Design Using CFD and Control Theory," AIAA Paper 95–1729, AIAA 12th Computational Fluid Dynamics Conference, San Diego, California, june 1995.

[5]Fransson, T. H., private communication, Laboratoire de Thermique appliquee et Turbomachines, Ecole Polytechnique Federale de Lausanne, Lausanne, Switzerland, 1991.

[6]Hall, K. C. and Clark, W. S., "Linearized Euler Predictions of Unsteady Aerodynamic Loads in Cascades," *AIAA Journal*, Vol. 31, No. 3, March 1993, pp. 540–550.

[7]"Workshop on 2D and 3D Flow Calculations in Turbine Bladings," Tech. Rep. 1982-05, Von Karman Institue for Fluid Dynamics, april 1982.

[8]Eyi, S. and Lee, K. D., "Transonic Turbomachinery Blade Design Using Optimization," AIAA Paper 1997-0159, AIAA 35th Aerospace Sciences Meeting, Reno, Nevada, 1997.

[9]Yang, S., Wu, H., and Liu, F., "Aerodynamic Design of Cascades by Using an Adjoint Equation Method," AIAA Paper 2003-1068, AIAA 41st Aerospace Sciences Meeting, Reno, Nevada, 2003.

[10]Fletcher, R. and Reeves, C. M., "Function Minimization by Conjugate Gradients," *Comput J7*, 1964, pp. 149–154.

[11]Wang, L., "Transonic Airfoil Optimum Design Based on Control Theory," Thesis, Northwestern Polytechnical University, Xi'an, China, 1999.

[12]Jameson, A., "Aerodynamic Shape Optimization Using the Adjoint Method," Lecture series, Von Karman Institute for Fluid Dynamics, Feb. 2003.